Mon. Not. R. Astron. Soc. **000**, 000–000 (0000) Printed 23 May 2016 (MN LATEX style file v2.2)

Accretion mode of the Ultra-Luminous X-ray source M82 X-2

S. Karino[1⋆] and J. C. Miller[2]†
[1] *Faculty of Engineering, Kyushu Sangyo University, 2-3-1 Matsukadai, Fukuoka 813-8503, Japan*
[2] *Department of Physics (Astrophysics), University of Oxford, Keble Road, Oxford OX1 3RH, UK*

2016 May 7

arXiv:1605.05723v2 [astro-ph.HE] 20 May 2016

ABSTRACT

Periodic pulsations have been found in emission from the ultra-luminous X-ray source (ULX) M82 X-2, strongly suggesting that the emitter is a rotating neutron star rather than a black hole. However, the radiation mechanisms and accretion mode involved have not yet been clearly established. In this paper, we examine the applicability to this object of standard accretion modes for high mass X-ray binaries (HMXBs). We find that spherical wind accretion, which drives OB-type HMXBs, cannot apply here but that there is a natural explanation in terms of an extension of the picture for standard Be-type HMXBs. We show that a neutron star with a moderately strong magnetic field, accreting from a disc-shaped wind emitted by a Be-companion, could be compatible with the observed relation between spin and orbital period. A Roche lobe overflow picture is also possible under certain conditions.

Key words: accretion, accretion disk — stars: neutron — X-rays: binaries — X-rays: individuals: M82 X-2

1 INTRODUCTION

Ultra-luminous X-ray sources (ULXs) are very bright extragalactic X-ray point sources, with observed fluxes which would correspond to luminosities greater than 10^{39} ergs per second if they were radiating isotropically. Since this is above the Eddington limit for normal stellar-mass compact objects, it has been widely thought that they are associated with intermediate-mass black holes (IMBHs) (Farrell et al. 2009), although non-spherical accretion and beamed emission could give rise to inferred luminosities significantly above the Eddington limit (see, for example Ohsuga & Mineshige 2011), allowing also for lower masses.

Bachetti et al. (2014) have reported NuSTAR observations of ULX M82 X-2 (also known as NuSTAR J095551+6940.8) which reveal periodic changes in the hard X-ray luminosity of this source, indicative of a rotating magnetized neutron star being involved rather than a black hole. The measured peak flux (in the $3-30$keV band) would correspond to $L_X = 3.7 \times 10^{40}\,\mathrm{erg\,s^{-1}}$ if the radiation were isotropic, and is challenging to explain with a neutron star. The period (taken to be the neutron-star spin period) was found to be $P_\mathrm{s} = 1.37\,\mathrm{s}$, with a 2.53-day sinusoidal modulation, interpreted as being an orbital period P_orb corresponding to motion around an unseen companion which would be the mass donor in the accreting system. The time derivative of the spin period $\dot{P}_\mathrm{s}$ was also measured. Values for this coming from different individual observations show considerable variations but a relevant underlying spin-up tendency was found, with $\dot{P}_\mathrm{s} = -2 \times 10^{-10}\,\mathrm{s\,s^{-1}}$. The mass donor is indicated as having a mass larger than $5.2M_\odot$, so that the system should be categorized as a high mass X-ray binary (HMXB). Taking canonical neutron star parameters as a rough guide ($M_\mathrm{NS} = 1.4M_\odot$ and $R_\mathrm{NS} = 10\,\mathrm{km}$), the luminosity relation $L_\mathrm{X} = GM_\mathrm{NS}\dot{M}R_\mathrm{NS}^{-1}$, gives the mass accretion rate corresponding to $L_\mathrm{X} = 3.7 \times 10^{40}\mathrm{erg\,s^{-1}}$ as being $\dot{M} = 2.0 \times 10^{20}\mathrm{g\,s^{-1}} = 3.1 \times 10^{-6}\mathrm{M_\odot yr^{-1}}$.

There are three main mechanisms by which the mass transfer might occur: (i) via a spherical wind (as for O-type HMXBs), (ii) via a disc-shaped wind (as for Be-type HMXBs), or (iii) by Roche lobe overflow (RLOF). Because of the large inferred $\dot{M}$, the third option was suggested as the mechanism by Bachetti et al. (2014) and subsequent studies (Ekşi et al. 2015; Dall'Osso et al. 2015).

Here, we investigate each of these scenarios in turn to see which may be appropriate for ULX M82 X-2. In Section 2, we discuss the strength required for the neutron-star magnetic field, and show that it needs to be moderately strong but not at a magnetar level. In Section 3, we discuss the applicability of scenarios (i)-(iii), finding that (i) is excluded but that (ii) and (iii) could be viable possibilities. In Section

⋆ E-mail: karino@ip.kyusan-u.ac.jp
† E-mail: john.miller@physics.ox.ac.uk

4, we discuss the role of the propeller effect and transient behaviour, and Section 5 contains conclusions.

2 CLASSICAL ACCRETION ESTIMATES FOR THE NEUTRON-STAR MAGNETIC FIELD STRENGTH

In the standard picture for HMXBs, the system has to be fairly young because the companion donor star is massive enough to have only a rather short main-sequence life-time. Matter coming from the donor star falls towards its neutron star companion, becomes included in a Keplerian accretion disc, and eventually becomes entrained by the neutron star's magnetic field, creating hot X-ray emitting accretion columns above the magnetic poles (cf. Pringle & Rees 1972). Sufficiently young neutron stars typically have magnetic-field strengths above 10^{12} G (see, for example, the data in the ATNF pulsar catalogue, Manchester et al. 2005), with a tail of the distribution extending beyond 10^{13} G and eventually joining with the magnetar regime at 10^{14} G. This can be relevant for explaining how this source can be so luminous, because if the magnetic field is stronger than the quantum limit, $B > 4.4 \times 10^{13}$G, the scattering cross-section would be suppressed, reducing the opacity of matter in the accretion columns above the magnetic poles and allowing higher luminosities. With this in mind, Ekşi et al. (2015) suggested that this source might contain a magnetar. The computational results of Mushtukov et al. (2015) and the evidence of propeller effect from Tsygankov al. (2016) support this idea. In other works, however, Christodoulou et al. (2014), Lyutikov (2014) and Dall'Osso et al. (2015) have explored different scenarios with standard pulsar fields $\sim 10^{12} - 10^{13}$G, while other authors have advocated weaker fields, $\sim 10^{9}$G (Kluźniak & Lasota 2015; Tong 2014). As the present work was being completed, we have seen a new paper by King & Lasota (2016), advocating a model with strong beaming and a magnetic field of $\sim 10^{11}$G. The work presented here represents a line of study parallel to theirs.

We focus here on a scenario with a field at the top end of the range for standard pulsars. In the rest of this section, we apply some simple assumptions for testing the relevance of a solution of this type.

We take the full entrainment of the accreting matter by the magnetic field to occur close to the magnetic radius, $r_{\rm m}$, where the magnetic pressure balances the ram pressure of the infalling matter. Using the condition of mass continuity, we then obtain the following expression for the magnetic radius:

$$r_{\rm m}^7 = \frac{B_{\rm NS}^4 R_{\rm NS}^{12}}{8\zeta^2 G M_{\rm NS} \dot{M}^2}. \tag{1}$$

Here $B_{\rm NS}$ is the field strength at the surface of the neutron star, and ζ is the ratio of the accretion velocity to the free-fall velocity (Waters & van Kerkwijk 1989). At $r = r_{\rm m}$, the accreting matter is taken to come into corotation with the neutron star, with the corotation speed being $v_{\rm corot} = 2\pi r_{\rm m} P_{\rm s}^{-1}$. Since the system is probably close to spin equilibrium (Bachetti et al. 2014; Dall'Osso et al. 2015), it is reasonable to take $v_{\rm corot}$ as being approximately equal to the Keplerian velocity at $r = r_{\rm m}$. We can then estimate the appropriate value of the field strength in order to be consistent with the observed spin period for ULX M82 X-2. This gives

$$\begin{aligned} B_{\rm NS} &= 2^{-5/12}\pi^{-7/6}\zeta^{1/2}G^{5/6}M_{\rm NS}^{5/6}R_{\rm NS}^{-3}\dot{M}^{1/2}P_{\rm s}^{7/6} \\ &= 4.46\times10^{13}{\rm G} \\ &\quad\times\zeta^{1/2}\left(\frac{M_{\rm NS}}{1.4M_\odot}\right)^{5/6}\left(\frac{R_{\rm NS}}{10^6{\rm cm}}\right)^{-3} \\ &\quad\times\left(\frac{\dot{M}}{2.0\times10^{20}{\rm g\,s^{-1}}}\right)^{1/2}\left(\frac{P_{\rm s}}{1.37{\rm s}}\right)^{7/6}. \end{aligned} \tag{2}$$

Interestingly, this value is just above the critical quantum limit $B_{\rm crit}$ at which electron scattering is suppressed, as mentioned earlier:

$$B_{\rm crit} = \frac{m_{\rm e}^2 c^3}{\hbar e} = 4.4\times10^{13}{\rm G} \tag{3}$$

(Ekşi et al. 2015).

On the other hand, we can also consider the spin-up rate, focusing on the measured underlying tendency $\dot{P}_{\rm s} = -2\times10^{10}{\rm s\,s^{-1}}$ (Bachetti et al. 2014), rather on the variations seen in the individual measurements, as mentioned earlier. We use the classical Ghosh & Lamb model (Ghosh & Lamb 1979), in order to identify appropriate parameter values; the spin-up rate is then given by Eq. (15) in their paper. Assuming that the moment of inertia of the neutron star has the canonical value, $10^{45}{\rm g\,cm^2}$, and using the spin-up rate given by Bachetti et al. (2014), we find that the magnetic field strength corresponding to $\dot{P}_{\rm s} = -2\times10^{-10}{\rm s\,s^{-1}}$ would be $B_{\rm NS}\left(\dot{P}_{\rm s} = -2\times10^{-10}\right) = 4\times10^{13}$G, which is very similar to the value obtained above, in Eq. (2), from considerations of the spin period.

Based on these two independent estimates, we conclude that having a field of $\sim 4\times10^{13}$G can be consistent with the interpretation that M82 X-2 could be an example (albeit a rather extreme one) of previously-known classes of HMXBs (see, for example, Klus et al. (2014)). A field of this strength can be just large enough to permit the quantum suppression of electron scattering as invoked by Ekşi et al. (2015).

3 THE ACCRETION MODE OF ULX M82 X-2

In this section, we examine the different possibilities mentioned in the Introduction for the accretion mode of ULX M82 X-2. The two mechanisms operating for standard HMXBs are: (i) accretion from a spherical wind emitted by the donor star, and (ii) accretion from a disc-shaped wind, thought to come from a "decretion disc" around the donor star (in a decretion disc, angular momentum is continually added to the inner edge of the disc from the rapidly rotating central star, and the matter drifts outwards rather than inwards). Type (i) occurs for OB-type HMXBs, while type (ii) fuels Be-type HMXBs. Additionally, although there is no observational evidence for this in standard HMXB studies, it is possible that Roche lobe overflow (RLOF) could be relevant here; we are referring to this as type (iii). Bachetti et al. (2014) and Ekşi et al. (2015) both suggested RLOF as a likely accretion mode for M82 X-2, but did not discuss it in detail. In a recent paper, however, Shao & Li (2015) presented an argument suggesting that a certain proportion of ULXs should indeed be accreting neutron stars with RLOF mass-transfer. Here, we will consider each of the mechanisms in turn to assess which of them may be appropriate

for our case. In order to give a luminosity as high as that observed, the accretion rate needs to be at least as high as $\dot{M} \sim 10^{-6} M_{\odot} \mathrm{yr}^{-1}$, as shown earlier.

3.1 Accretion fed from a spherical wind

First, we consider whether a spherical stellar wind coming from the massive donor could successfully fuel ULX M82 X-2 (type (i) accretion). In simple stellar wind models, the wind velocity is frequently described by an expression of the form

$$v_{\mathrm{w}}(r) = v_{\infty}\left(1 - \frac{R_*}{r}\right)^{\beta} \tag{4}$$

(Kudritzki & Plus 2000), where v_{∞} is the terminal velocity of the wind, R_* is the stellar radius, r is the distance from the centre of the donor star, and β is a parameter whose value is close to unity (we will take $\beta = 1$ exactly here). The accretion rate from a spherical wind is usually described by the Hoyle-Lyttleton formula (Hoyle & Lyttleton 1939):

$$\dot{M} = \rho_{\mathrm{w}} v_{\mathrm{rel}} \pi R_{\mathrm{acc}}^2, \tag{5}$$

where R_{acc} is the accretion radius defined by

$$R_{\mathrm{acc}} = \frac{2GM_{\mathrm{NS}}}{v_{\mathrm{rel}}^2}, \tag{6}$$

and v_{rel} is the velocity of the neutron star relative to the accreting matter: $v_{\mathrm{rel}}^2 = v_{\mathrm{w}}^2 + v_{\mathrm{orb}}^2$, where v_{orb} is the orbital velocity of the neutron star. The wind density can be written as

$$\rho_{\mathrm{w}}(r) = \frac{\dot{m}_{\mathrm{w}}}{4\pi r^2 v_{\mathrm{w}}}, \tag{7}$$

where $\dot{m}_{\mathrm{w}}$ is the rate of mass loss from the donor star. If one specifies a particular value for $\dot{m}_{\mathrm{w}}$, the accretion rate $\dot{M}$ can be calculated from Eq. (5), and then the corresponding X-ray luminosity of the neutron star can be obtained from $L_{\mathrm{X}} = GM_{\mathrm{NS}}\dot{M}R_{\mathrm{NS}}^{-1}$.

Vink et al. (2001) have given analytic formulae from which $\dot{m}_{\mathrm{w}}$ can be calculated for high-mass stars in terms of their mass M_*, luminosity L_*, effective temperature T_{eff} and the ratio $v_{\infty}/v_{\mathrm{esc}}$, where v_{∞} is the wind's terminal velocity and v_{esc} is the escape velocity from the stellar surface. A change in behaviour occurs when T_{eff} passes a value $T_{\mathrm{crit}} \approx 25000$K and separate formulae are given for temperatures above and below that. Here we use the mass loss rates given by equations (24) and (25) in their paper. The ratio $v_{\infty}/v_{\mathrm{esc}}$ is known to be ~ 2.6 for $T_{\mathrm{eff}} > T_{\mathrm{crit}}$ and ~ 1.3 for $T_{\mathrm{eff}} < T_{\mathrm{crit}}$ (Lamers et al. 1995; Vink et al. 2001) while values for L_* and T_{eff} can be obtained as functions of M_* using a stellar evolution code (we used the analytic fitting formulae from the paper by Hurley et al. (2000)). Putting this data into Eqs. (5) – (7), we could then calculate predicted values of the X-ray luminosity for a sequence of masses of the donor star, and our results are shown in Fig. 1.

The two curves in Fig. 1 correspond to different evolutionary phases; the zero-age main sequence phase (solid curve) and the terminal main sequence phase (dashed curve). For stars more massive than 30 $M_{\odot}$, the stellar radius becomes larger than that of the binary orbit,

$$a = \left[\frac{P_{\mathrm{orb}}^2}{4\pi^2} G\left(M_1 + M_{\mathrm{NS}}\right)\right]^{1/3}, \tag{8}$$

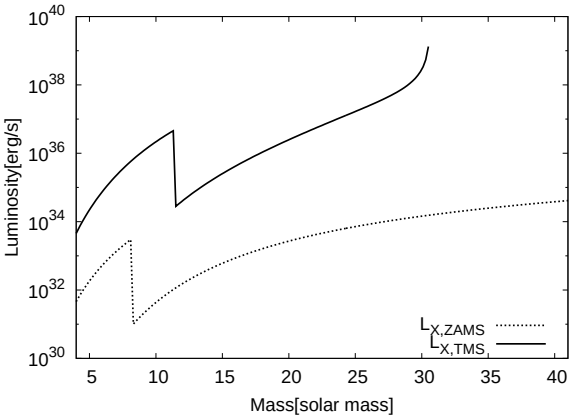

Figure 1. Predicted X-ray luminosities are shown as functions of the mass of the donor star, assuming spherical wind accretion. The different curves correspond to different evolutionary phases: the zero-age main sequence phase (ZAMS, dashed curve) and the terminal main sequence phase (TMS, solid curve).

before it reaches the terminal main sequence (here M_1 is the mass of the donor star). It is clear, from this figure, that even if we consider the most efficient conditions, and an optimal viewing angle, an X-ray luminosity of ULX level ($L_{\mathrm{X}} \simeq 10^{40}$) cannot be achieved. Hence, we conclude that ULX M87 X-2 cannot be fed by a spherical wind because the density of the wind would not be high enough.

3.2 Accretion fed by a decretion-disc wind coming from around a Be star

The Corbet diagram (where P_{orb} is plotted against P_{s}) is frequently used in studies of HMXBs, and it can be useful to consider it also in the present context. OB-type and Be-type HMXBs show clearly different distributions in these diagrams, with the majority of the Be-type ones being close to the diagonal from lower-left to upper-right (they are the points marked with a + in Fig. 2). Waters & van Kerkwijk (1989) obtained an expression for the sequence followed by the Be-type HMXBs by assuming the Hoyle-Lyttleton accretion rate given by Eq. (5). The decretion disc wind parameters ρ_{w} and v_{w} could be taken from any appropriate wind model; Waters & van Kerkwijk (1989) adopted a simple disc-shaped model:

$$\rho(r) = \rho_0 \left(\frac{r}{R_{\mathrm{Be}}}\right)^{-n}, \tag{9}$$

$$v(r) = v_0 \left(\frac{r}{R_{\mathrm{Be}}}\right)^{n-2}, \tag{10}$$

where ρ_0 and v_0 are the density and velocity at the stellar radius R_{Be}, and n is a constant which needs to be fixed. In order to explain the positions of known standard Be-HMXBs in the Corbet diagram, Waters & van Kerkwijk (1989) used $n = 3.25$, and we will also use this value in the following. This choice is roughly consistent with recent numerical computations of Be-disc winds (Krtička et al. 2011; Carciofi et al. 2012). With this wind model and any specified value of the magnetic field strength, one can obtain a corresponding relationship between P_{s} and P_{orb} by substi-

tuting equation (5) into equation (2) ($P_{\rm orb}$ is related to a via equation (8)). This gives

$$P_{\rm s} = C \left(\frac{v_{\rm w}}{v_{\rm rel}}\right)^{-9/7} \left(\frac{\pi\rho_0}{v_0^3}\right)^{-3/7} \left(\frac{a}{R_{\rm Be}}\right)^{3(4n-6)/7}, \qquad (11)$$

where

$$C = 2^{15/14}\pi \left(B_0 R_{\rm NS}^3\right)^{6/7} (2GM_{\rm NS})^{-11/7}. \qquad (12)$$

In Fig. 2 we show $P_{\rm orb}$-$P_{\rm s}$ curves, obtained from Eq. (11), for three values of both B and ρ_0. The values used for v_0 and the radius of the neutron star are the same as those used by Waters & van Kerkwijk (1989): $v_0 = 10^6 {\rm cm\,s^{-1}}$ and $R_{\rm NS} = 10^6 {\rm cm}$. In the two frames, we show the results for two different donor masses: $6M_\odot$ and $12M_\odot$, with the corresponding radii being those for the terminal main sequence phase on the stellar evolution tracks of Hurley et al. (2000): $R_{\rm Be} = 10.7R_\odot$ for the $12M_\odot$ donor and $R_{\rm Be} = 6.8R_\odot$ for the $6M_\odot$ donor. It can be seen that the results in the two frames are very similar. In each of them, ULX M82 X-2 (marked with the circles) takes a rather extreme position in comparison with the Be-HMXBs but, for an appropriate set of parameters, it does fit with the Be-HMXB sequences. As shown in the figure, assuming a magnetic field strength of $B = 4 \times 10^{13}$G, the model given by Eq. (11) with the density $\rho_0 = 2 - 3 \times 10^{-10} {\rm g\,cm^{-3}}$ does fit the position of ULX M82 X-2 very well in both cases.

Of course, the position of ULX M82 X-2 on the figure could also be explained by models with lower B and extremely low ρ_0, or higher B and extremely high ρ_0. From the limited available polarization data, Draper et al. (2014) suggested that the ρ_0 for discs around Be-stars is between 8×10^{-11} and $4 \times 10^{-12} {\rm g\,cm^{-3}}$, based on the nine systems which they studied. Touhami et al. (2011) tested values of ρ_0 between 2×10^{-12} and $2 \times 10^{-10} {\rm g\,cm^{-3}}$ for fitting the IR radiation from Be discs, and suggested that the best fit value is $1.4 \times 10^{-10} {\rm g\,cm^{-3}}$. In view of these results, our best fit density ($\rho_0 = 2 \times 10^{-10} {\rm g\,cm^{-3}}$) seems slightly high but still a reasonable value. Additionally, if we take this value for ρ_0, Eq. (5) gives $3.2 \times 10^{20} {\rm g\,s^{-1}}$ for the mass accretion rate which is again quite reasonable for ULX M82 X-2. We note that a field as low as $\sim 10^{11}$G would be difficult to accommodate within this picture.

With this large mass loss rate, however, the donor Be-star cannot maintain a high density disc for very long and so, after the bright (high accretion rate) phase, it would run out of decretion disc matter. Hence, in this scenario, the accreting system would inevitably become a transient. Since, according to the archival survey, ULX M82 X-2 does show transient tendencies, this prediction seems to be consistent with the observations (Doroshenko et al. 2014). We note, however, that transient behaviour could also be understood in the context of propeller switching (Tsygankov al. 2016), as we will discuss later.

3.3 Roche lobe overflow

Bachetti et al. (2014) suggested that the accretion mode for ULX M82 X-2 may involve Roche lobe overflow (RLOF) and we need to consider this scenario as well.

An approximate value for the Roche radius $R_{\rm RL}$ is given by

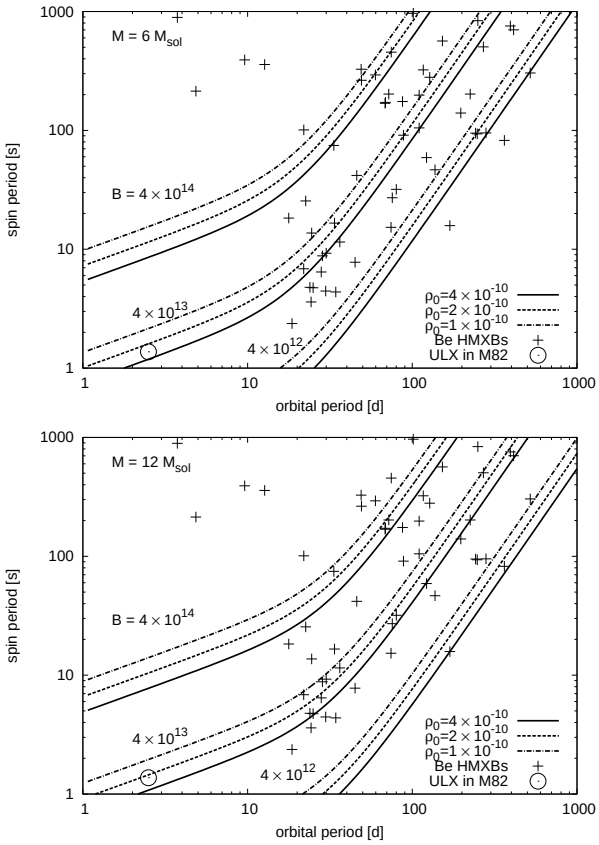

Figure 2. The Corbet diagram, showing the orbital period of the binary system $P_{\rm orb}$ plotted against the spin period of the neutron star $P_{\rm s}$. The upper and lower panels show results for donor masses of $6M_\odot$ and $12M_\odot$, respectively. The $P_{\rm orb}$-$P_{\rm s}$ relation given by equation (11) is shown by the continuous curves with the three sets of curves in each panel showing results for different values of B (measured in gauss), and the different curves of each set being for different disc densities (in ${\rm g\,cm^{-3}}$). The stellar radii are set to the terminal main sequence values obtained from the stellar evolution tracks of Hurley et al. (2000). The positions on the diagram of known standard Be-type HMXBs are shown with crosses, while that for ULX M82 X-2 is shown with a circle. The data for the Be-HMXBs is taken from Karino (2007) and Klus et al. (2014).

$$R_{\rm RL} = \frac{0.49q^{2/3}}{0.6q^{2/3} + \ln\left(1 + q^{1/3}\right)} a \qquad (13)$$

(Eggleton 1983), where q is the mass ratio $M_1/M_{\rm NS}$ (with M_1 being the mass of the donor star) and a is an orbital separation given by Eq. (8). For having RLOF accretion, the donor radius needs to be larger than the Roche radius but smaller than the orbital radius. Fig. 3 shows evolutionary tracks for the radii of stars with selected masses (again using data from Hurley et al. (2000)) with the dotted lines linking the points where each track crosses its corresponding Roche radius (lower curve) and orbital radius (upper curve). The shaded region in Fig. 4 shows where RLOF can occur and is plotted as a function of the mass of the donor star. The upper bound of this shaded region corresponds to the orbital radius, and the lower bound shows the Roche radius. Stellar radii at several evolutionary stages (zero-age main sequence, the end of the main sequence and the beginning of the giant branch) are also shown.

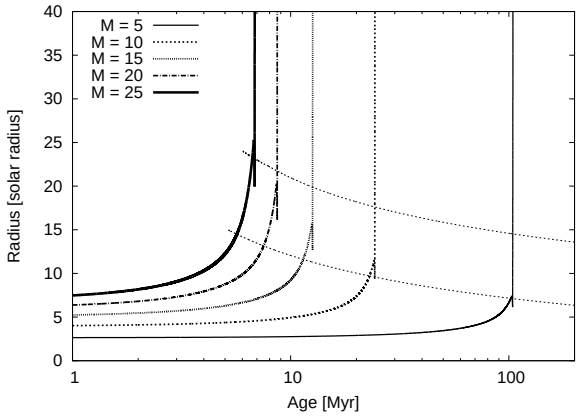

Figure 3. The radii of potential donor stars, with selected masses, are plotted as a function of their age. Each track starts from the zero-age main sequence and terminates at the starting point of the giant branch. The dotted curves link the points where each track crosses its corresponding Roche radius (lower curve) and orbital radius (upper curve). Data from Hurley et al. (2000).

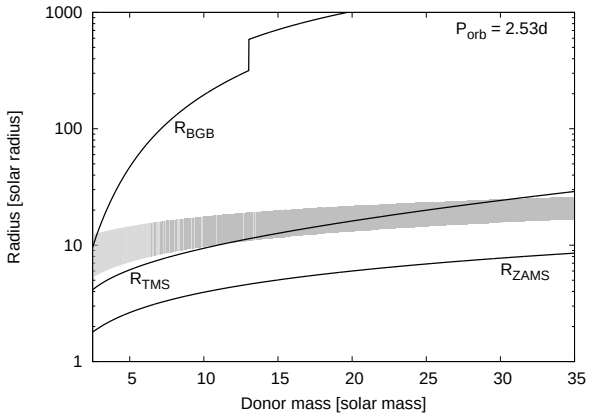

Figure 4. Relevant radii are plotted as functions of the mass of the donor star. The Roche lobe radius and orbital radius are shown bounding the shaded region below and above, respectively. The radii of potential donor stars are shown at various evolutionary stages: on the zero-age main sequence (lower curve), the end of the main sequence (middle curve) and the beginning of the giant branch (upper curve). The data are taken from equations (1) – (30) of Hurley et al. (2000).

If M_1 is larger than $11M_\odot$, the donor star already fills its Roche lobe during the main sequence stage, leading to the type of mass transfer known as Case A (Paczyński 1971). This occurs on the thermal timescale

$$\tau_{\rm th} \sim \frac{GM^2}{RL}. \qquad (14)$$

For a massive star, this timescale is shorter than 10^6yr and the mass transfer rate reaches $10^{-5}M_\odot{\rm yr}^{-1}$, which is sufficient for feeding ULX M87 X-2. However, for the most massive stars ($M \geqslant 30M_\odot$), the main-sequence stellar radius would be larger than the orbital radius as well, so that a common envelope would form around the binary in a short time scale. In that case, the system would be luminous at infra-red frequencies rather than in X-rays (Ivanova et al. 2013); the donor must therefore be less massive than this in order to give the right sort of RLOF accretion. Furthermore, the mass of the donor ought to be restricted by the fact that the companion is a neutron star: the progenitor of the neutron star would have been the primary when this binary system was born and, according to Fryer (1999), it should have had an original mass of less than $20-30M_\odot$ in order to give rise to a neutron star rather than a black hole. The present primary should be less massive than the original one (even if its mass may have increased slightly during the first mass transfer stage), and hence the donor mass is constrained to be less than roughly $\sim 25M_\odot$.

Another issue which needs to be taken into account is that if the mass ratio $q = M_1/M_{\rm NS}$ is above a certain limit (~ 5 for a red giant, and ~ 12 for a high-mass main sequence star), the binary would be subject to the Darwin instability, meaning that it could not sustain a circular orbit as required in order for RLOF to be a viable candidate mechanism here (Counselman 1973; Eggleton 2006).

For M_1 between $\sim 5-11M_\odot$, the star will be inside its Roche lobe during its main sequence lifetime but may overflow it during its expansion at the end of the main sequence (Hertzsprung gap phase), giving an early Case B type of mass transfer. This also proceeds on the thermal timescale, as given above, and could in principle be sufficient to feed ULX M87 X-2. However, in general the timescale on which the star crosses the Hertzsprung gap is quite short. For instance, an $8M_\odot$ star evolves from the end of the main sequence to the giant branch in 0.35 Myr (Eggleton 2006) and would have a radius between $R_{\rm RL}$ and a for only some fraction of that (determining which would require a detailed stellar evolution calculation). The relevant time is then very short compared with the overall life-time of the star ($\sim$ 40Myr for $8M_\odot$). However, the duration of the Hertzsprung gap phase depends sensitively on the mass of the donor star and for the minimum donor mass envisaged, $5.2M_\odot$ (Bachetti et al. 2014), it becomes $\sim$ 1.5Myr. While it would still require a lucky chance to see any ULX fed by this Case B type of RLOF accretion, it would become less unlikely with the least massive possible donor stars. In connection with this: according to the population synthesis simulation of Shao & Li (2015), the number of ULXs containing a neutron star should peak for systems having donor stars in a small mass range around $6-8M_\odot$, and so it is possible that the short ULX lifetime of these systems could be compensated by there being so many of them, and that they might actually predominate in the observations.

To summarise: accretion via RLOF might possibly be the mechanism for ULX M82 X-2 if the donor is an evolved star of $\sim 5-8\,M_\odot$ passing through the Hertzsprung gap. An RLOF scenario with a main sequence donor of $\sim 12-20\,M_\odot$ could also be a possibility although, for the higher masses, such a system would be prone to the orbit becoming eccentric due to the Darwin instability. An RLOF scenario with the donor being evolved up to the giant phase is ruled out completely.

4 SOME FURTHER ISSUES

In the previous sections, we have discussed similarities between ULX M82 X-2 and known standard HMXBs, in terms of the strength of the neutron star's magnetic field and the

accretion mode. In Section 2, we concluded that a fairly strong magnetic field, of around 4×10^{13}G is favoured for this object. While our considerations have been quite simple ones, this conclusion is consistent with more detailed analyses (Ekşi et al. 2015; Dall'Osso et al. 2015). In Section 3, we considered the possible feeding mechanisms, concluding that accretion modes similar to those of standard Be-HMXBs are possible here, and that some mechanisms involving Roche lobe overflow would also be possible. In the present section, we discuss two further related issues.

4.1 Propeller effect and transient behaviour

The 1.37 second spin period of the neutron star in ULX M82 X-2 is shorter than those of most HMXBs (which are typically in the range of $\sim 10 - 100$s). In view of this and the rather high magnetic field which we are inferring, one needs to consider whether it would be able to continue accreting matter from its disc, and continue to spin up, or whether it would enter the propeller regime where the disc matter is instead forced away (Illarionov & Sunyaev 1975). The critical period for onset of the propeller regime is given by

$$P_{\rm s,crit} = 81.5 \mu_{30}^{16/21} L_{\rm X,36}^{-5/7}, \quad (15)$$

where μ_{30} is the magnetic moment measured in units of 10^{30}G cm^3, as before, and $L_{\rm X,36}$ is the X-ray luminosity in units of 10^{36}erg s^{-1} (Ikhsanov 2003; Raguzova & Popov 2005). Fig. 5 shows the spin period - luminosity plane, with the straight lines marking the relation given by Eq. (15) for various values of B. Also shown are the locations on the plot of known HMXBs (marked with crosses) and of ULX M82 X-2 (marked with the circle). For the latter, we are taking the values $P_{\rm s} = 1.37$s and $L_{\rm X} = 3.7 \times 10^{40}$erg s^{-1}. Below the line for the relevant value of B, the propeller regime is operative; above it, accretion can proceed. According to this, ULX M82 X-2 would avoid the propeller regime if it has $B < 9.0 \times 10^{13}$G and so field strengths between the quantum limit of 4.4×10^{13}G and the maximum of 9.0×10^{13}G could give accretion and spin-up, but magnetar-strength fields of above 10^{14}G could not do so. The allowed range for B to exceed the quantum critical limit but avoid the propeller effect, is small but non-vanishing.

It has been reported that archival data for M82 X-1/X-2 from XMM Newton shows only tiny fluctuations at a level below 2.2 % (Doroshenko et al. 2014). This could be understood in two different ways. Firstly, the pulsations seen by Bachetti et al. (2014) could be a transient behaviour so that while XMM Newton did not see the pulsations during the time-span of its observations, NuSTAR did see them. The second possibility is that the pulsations might be observable only in the high energy range above 10 keV, so that NuSTAR could detect them while XMM Newton could not. Dall'Osso et al. (2015), noting the variations seen by Bachetti et al. (2014) in different measurements of $\dot{P}_{\rm s}$, have suggested that the system may be marginal for exhibiting the propeller effect, switching it on and off, and that the strong X-ray emissions and pulsations may only be observed when the propeller mechanism is not operating whereas during the propeller phase, only radiation from the hot disc is seen. In their latest and more extended analysis (Dall'Osso et al. 2016), they conclude that the magnetically threaded disc model with $B \sim 10^{13}$G could explain the observed properties of this object very well. Tsygankov al. (2016) also argue that the observed bimodal distribution of X-ray luminosity can be interpreted as being due to the propeller effect switching on and off. In their picture, even when the system is in the propeller regime, a small fraction of matter still leaks through the magnetic field lines and continues to give rise to lower luminosity emission.

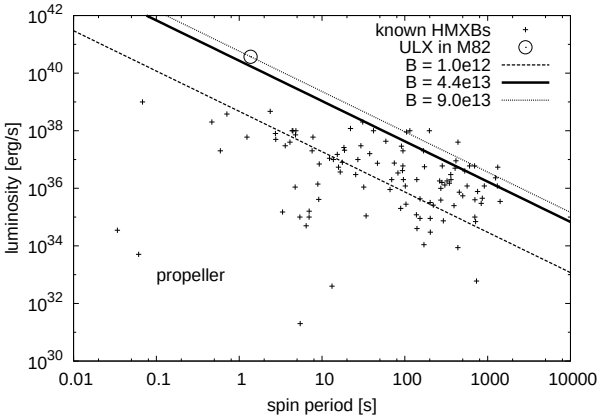

Figure 5. The locations of ULX M82 X-2 and known HMXBs in the spin-period - luminosity plane. The critical lines of the propeller transition, for $B = 10^{12}$G (dashed), 4.4×10^{13}G (thick solid) and 9.0×10^{13}G (dotted) are shown. To avoid the propeller effect operating, the location of ULX M82 X-2 needs to be above the line corresponding the surface magnetic field strength of its neutron star, i.e. B needs to be smaller than 9.0×10^{13}G for the parameter values given in the text, which is nevertheless significantly greater than the quantum limit $B \sim 4.4 \times 10^{13}$G.

Another point is that HMXBs can often show different pulsation behaviour in different energy ranges, with the higher energy X-rays being emitted as a *pencil beam*, while lower energy ones are emitted as a *fan beam* (Basko & Sunyaev 1975). In this case, the emission directions would be different for the different energy ranges. In fact, more than 20% of HMXBs show different light-curve shapes in high and low energy bands (Karino 2007). At present, the discussion on the transient behavior of M82 X-2 cannot be concluded at all. More data is needed for deciding between these different possibilities.

4.2 X-ray irradiation

Also one needs to consider the effect of irradiation of the accreting matter by the strong X-ray emission coming from the neutron star. The direct effect of the radiation pressure coming from this is, of course, to act as another obstacle for the accretion. In order to achieve a high accretion rate in luminous X-ray systems, some means is required for avoiding this obstacle, such as anisotropy of the X-ray radiation (see, for example, Christodoulou et al. 2014; King & Lasota 2016). In the wind accretion case, however, there are effects of the irradiation which act in the opposite direction, enhancing the accretion rate onto the neutron star. In detached wind-fed binaries, intra-binary matter cannot avoid some photo dissociation under these circumstances, and this reduces the efficiency of the acceleration mechanism driving the line-accelerated stellar wind away from the donor star (Stevens & Kallman 1990; Watanabe et al. 2006;

Karino 2014). From equation (6) one can see that the resulting slower wind velocity would cause the accretion radius to be larger, and lead to *increasing* the accretion rate onto the neutron star, as given by equation (5). However, the wind velocity is limited by $(v_{\rm esc}^2 + v_{\rm orb}^2)^{1/2}$, where $v_{\rm esc}$ is the escape velocity at the donor surface, and so it cannot be slow enough to significantly affect our discussion here. Another potential positive effect of X-ray irradiation is that it could in principle cause the Roche lobe to become swamped with heated outer-envelope matter which could then overflow the Roche lobe even if the stellar radius was smaller than Roche radius (Iben et al. 1997). This would require very strong irradiation though; it could only work in tight systems with orbital periods of a few hours, and would not play any significant role for M82 X-2.

5 CONCLUSIONS

In this paper, we have discussed the magnetic field strength and accretion mode for the recently identified neutron star in the source ULX M82 X-2.

We have considered the conditions required for producing the observed values of the key parameters: $P_{\rm s} = 1.37$s, $L_{\rm X} = 3.7 \times 10^{40} {\rm erg\,s^{-1}}$, $P_{\rm orb} = 2.53$d and $\dot{P}_{\rm s} = -2 \times 10^{-10} {\rm s\,s^{-1}}$, and have argued that a consistent explanation can be given involving a moderately strong magnetic field at around the quantum limit $B \approx 4 \times 10^{13}$G. Having a field strength above the quantum limit is favourable for explaining the high observed luminosity, because of the reduced opacity in this case. However, we note that there have been a number of other suggestions regarding the magnetic field strength (Christodoulou et al. 2014; Dall'Osso et al. 2015, 2016; Ekşi et al. 2015; Kluźniak & Lasota 2015; Lyutikov 2014; Tong 2014); further observations and discussions are required for resolving the issue.

We then went on to examine whether the standard accretion modes for HMXBs can be appropriate for this object. We concluded that spherical wind accretion, which drives OB-type HMXBs, cannot be the mechanism here but that an extension of the standard mechanism for Be-type HMXBs can provide a natural explanation. We have shown that if the neutron star has a moderately strong magnetic field ($B \sim 4 \times 10^{13}$G) and there is wind accretion from a reasonably high-density ($\rho_0 = 2 - 3 \times 10^{-10} {\rm g\,cm^{-3}}$) decretion disc around the Be-companion, then all of the main properties of ULX M82 X-2, including its position on the Corbet diagram, would be consistent with the relations followed by standard Be-HMXBs. Roche lobe overflow accretion is also a possibility. If the donor star has sufficiently high mass, it should still be on the main sequence and Case A RLOF accretion could then feed the ULX; if it has lower mass, it would need to be undergoing Case B RLOF while passing through the Hertzsprung gap during its post-main-sequence expansion.

ACKNOWLEDGMENTS

We gratefully acknowledge helpful discussions with Odele Straub and Hitoshi Yamaoka during the course of this work.

REFERENCES

Bachetti, M. et al., 2014, Nature, 514, 202
Basko, M. M. & Sunyaev, R. A., 1975, A & A, 42, 315
Carciofi, A. C., Bjorkman, J. E., Otero, S. A., Okazaki, A. T., Štefl, S., Rivinius, T., Baade, D. & Haubois, X., 2012, ApJ, 744, 15
Christodoulou, D. M., Laycock, S. G. T. & Kazanas, D., 2014, preprint (arXiv:1411.5434)
Corbet, R. H. D., 1984, A & A, 141, 91
Corbet, R. H. D., 1986, MNRAS, 220, 1047
Counselman III, C. C., 1973, ApJ, 180, 307
Dall'Osso, S, Perna, R. & Stella, L., 2015, MNRAS, 449, 2144
Dall'Osso, S., Perna, R., Papitto, A., Bozzo, E. & Stella, L., 2016, MNRAS, 457, 3076
Doroshenko, V., Santangelo, A. & Ducci, L., 2014, A & A, 579, 22
Draper, Z. H., Wisniewski, J. P., Bjorkman, K. S. et al., 2014, ApJ, 786, 120
Eggleton, P. P., 1983, ApJ, 268, 368
Eggleton, P. P., 2006, "Evolutionary processes in binary and multiple stars", Cambridge Univ. Press, Cambridge UK
Ekşi, K. Y., Andac, I. C., Cikintoglu, S., Gencali, A. A., Gungor, C. & Oztekin, F., 2015, MNRAS, 448, L40
Farrell, S. A., Webb, N. A., Barret, D., Godet, O. & Rodrigues, J. M., 2009, Nature, 460,73
Fryer, C. L., 1999, ApJ, 522, 413
Ghosh, P. & Lamb, F. K., 1979, ApJ, 234, 296
Hoyle, F. & Lyttleton, R. A., 1939, Proc. Camb. Phil. Soc., 112, 205
Hurley, J. R., Pols, O. R. & Tout, C. A., 2000, MNRAS, 315, 543
Iben, I., Jr., Tutukov, A. V. & Fedorova, A. V. 1997, ApJ, 486, 955
Ikhsanov, N. R., 2003, A & A, 399, 1147
Illarionov, A. F. & Sunyaev, R. A., 1975, A & A, 39, 185
Ivanova, N., Justham, S., Avendano Nandez, J. L., & Lombardi, J. C., 2013, Science, 339, 433
Karino, S., 2007, PASJ, 59, 961
Karino, S., 2014, PASJ, 66, 34
King, A. & Lasota, J.-P., 2016, MNRAS, 458, 10
Kluźniak, W. & Lasota, J.-P., 2015, MNRAS, 448, L43
Klus, H., Ho, W. C. G., Coe, M. J., Corbet, R. H. D & Townsend, L. J., 2014, MNRAS, 437, 3863
Krtička, J., Owocki, S. P. & Meynet, G., 2011, A & A, 527, 84
Kudritzki, R.-P., & Plus, J., 2000, ARA & A, 38, 613
Lamers, H. G. L. M., Snow, T. P. & Lindholm, D. M., 1995, ApJ, 455, 269
Lépine, S. & Moffat, A. F. J., 2008, AJ, 136,548
Lyutikov, M., 2014, preprint (arXiv:1410.8745)
Manchester, R. N., Hobbs, G. B., Teoh, A. & Hobbs, M., 2005, AJ, 129, 1993, http://www.atnf.csiro.au/people/pulsar/psrcat/
Mushtukov, A. A., Suleimanov, V. F., Tsygankov, S. S. & Poutanen, J., 2015, MNRAS, 454, 2539
Ohsuga, K. & Mineshige, S., 2011, ApJ, 736, 2
Paczyński, B., 1971, ARA & A, 9, 183
Pringle, J. E. & Rees, M. J., 1972, A & A, 21, 1
Raguzova, N. V., & Popov, S. B., 2005, Astron. Astrophys.

Trans., 24, 151
Shao, Y. & Li, X. D., 2015, ApJ, 802, 131
Stevens, I. R. & Kallman, T. R., 1990, ApJ, 365, 321
Tong, H., 2015, Resarch in Astronomy and Astrophysics, 15, 517
Touhami, Y., Gies, D. R. & Schaefer, G. H., 2011, ApJ, 729, 17
Tsygankov, S. S., Mushtukov, A. A., Suleimanov, V. F. & Poutanen, J., 2016, MNRAS, 457, 1101
Vink, J. S., de Koter, A. & Lamers, H. G. L. M., 2001, A & A, 369, 574
Watanabe, S., Sako, M., Ishida, M., Ichisaki, Y., Kahn, S. M., Kohmura, T., Nagase, F., Paerels, F. & Takahashi, T., 2006, ApJ, 651, 421
Waters, L. B. F. M. & van Kerkwijk, M. H., 1989, A & A, 223, 196